NUKLEONIKA 2012;57(2):249–252

ORIGINAL PAPER

Multi-DBD actuator with floating inter-electrode for aerodynamic control

**Artur Berendt,
Janusz Podliński,
Jerzy Mizeraczyk**

Abstract. In this paper the use of a floating inter-electrode in a multi-DBD (dielectric barrier discharge) plasma actuator is described. The multi-DBD plasma actuators with floating inter-electrodes were investigated to get a longer DBD on a dielectric surface and to maximise generated net airflow. Our actuator was used to control the boundary layer flow separation around NACA0012 airfoil model. The results of our investigations suggests that multi-DBD actuators with floating inter-electrodes can be attractive for aerodynamic purposes.

Key words: plasma • surface dielectric barrier discharge • plasma actuator • airflow control

A. Berendt✉, J. Podliński
Centre for Plasma and Laser Engineering,
The Szewalski Institute of Fluid-Flow Machinery,
Polish Academy of Sciences,
14 Fiszera Str., 80-952 Gdańsk, Poland,
Tel.: +48 58 699 5122, Fax: +48 58 341 6144,
E-mail: aberendt@imp.gda.pl

J. Mizeraczyk
Centre for Plasma and Laser Engineering,
The Szewalski Institute of Fluid-Flow Machinery,
Polish Academy of Sciences,
14 Fiszera Str., 80-952 Gdańsk, Poland
and Department of Marine Electronics,
Gdynia Maritime University,
83 Morska Str., 81-225 Gdynia, Poland

Received: 22 September 2011
Accepted: 7 December 2011

Introduction

When a critical angle of attack of an airfoil is exceeded the boundary layer flow separation occurs (stall point). The lift coefficient of the airfoil rapidly decreases and a drag coefficient increases. The stall could lead to an autorotation of an aircraft and to fast reduction of an altitude. To prevent or postpone flow separation around airfoils many researches using DBD actuators were performed [3–5].

In this paper an innovative multi-DBD plasma actuator with floating inter-electrode is presented. The experimental results showed that this actuator could be attractive for aerodynamic applications, in particular for the leading edge flow separation control around NACA0012 airfoil model.

Experimental set-up

Our experiment was divided into two stages. In the first stage the innovative multi-DBD actuator with floating inter-electrodes was prepared and tested. The 2-D PIV (particle image velocimetry) measurements were performed in order to investigate airflow generation process in this actuator. In the second stage of the experiment ability of the multi-DBD actuator with floating inter-electrode for flow separation control around NACA0012 airfoil model was tested. For this purpose, the new multi-DBD actuator with a flexible dielectric barrier material was prepared and integrated with a NACA0012 airfoil model.

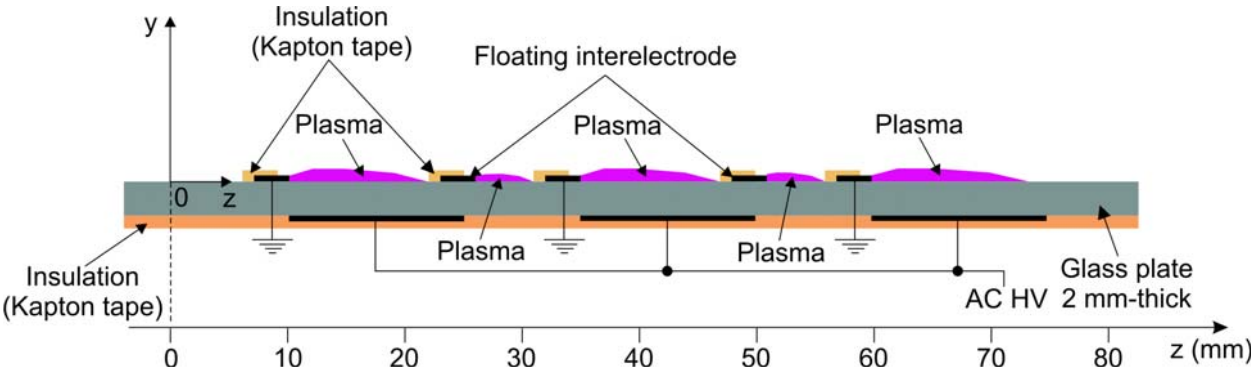

Fig. 1. Schematic side view of the multi-DBD actuator with floating inter-electrodes developed for airflow generation investigations.

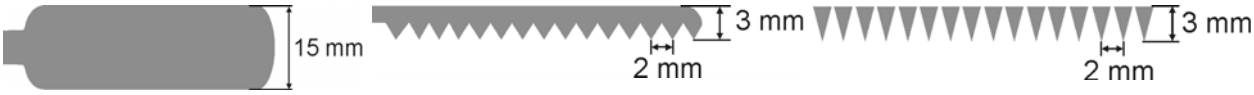

a b c

Fig. 2. Schematic top view of electrodes for multi-DBD actuator: smooth HV electrode (a), saw like grounded electrode (b), saw like floating inter-electrode (c).

The first stage of the experiment

The multi-DBD actuator with floating inter-electrodes used in the first stage of the experiment is presented in Fig. 1. It consisted of a 2 mm-thick glass plate (the electric relative permittivity $\varepsilon_r = 7$) and a smooth high voltage (HV) electrodes (Fig. 2a), a saw-like grounded electrodes (Fig. 2b) and floating inter-electrodes (Fig. 2c). As the floating inter-electrode, a series of separated copper teeth was used. All electrodes were made of a 50 μm-thick copper tape. The HV electrodes and the grounded electrodes were 50 mm long, while the length of floating inter-electrodes was 45 mm. The floating and the grounded electrodes were 3 mm wide and the HV electrodes were 15 mm wide. The partially insulated (only tips of the saw teeth were exposed to ambient air) floating and grounded electrodes were mounted on the upper side of the dielectric material, while the insulated HV electrodes were on the opposite side. The distances from the grounded electrodes to the floating inter-electrodes were 13 mm (e.g. from $z = 10$ mm to $z = 23$ mm). The distances from the floating inter-electrodes to the grounded electrodes were 6 mm (e.g. from $z = 26$ mm to $z = 32$ mm). There was no shift between grounded electrodes and high voltage electrodes. The floating inter-electrode saw teeth were shifted 1 mm with respect to a HV electrode edge.

The second stage of the experiment

Basing on the results obtained from the first stage of experiment, the new multi-DBD actuator with the floating inter-electrode for the boundary layer flow separation control experiment was developed (Fig. 3). In this case a flexible dielectric barrier (3 layers of a 45 μm-thick Kapton tape, the electric relative permittivity $\varepsilon_r = 3.5$) had to be used in order to integrate the actuator with the NACA airfoil model. The widths and shapes of the floating and grounded electrodes were the same as in the first stage of experiment (Figs. 2b and 2c) and the width of the smooth HV electrodes was 6 mm. All electrodes were 500 mm long. The distance from the first grounded electrode to the floating inter-electrode was 8 mm. The distance from the floating inter-electrode to the second grounded electrode was 3 mm. The shift between the grounded electrodes and the HV electrodes was 2 mm and the shift between saw teeth of the floating inter-electrode and the HV electrode edge was 1 mm.

The NACA0012 airfoil model with the integrated multi-DBD actuator was prepared for the leading edge flow separation control experiment. A cord of the airfoil was 200 mm and a span was 595 mm. The first discharge of the multi-DBD actuator started in position $z/C = 4\%$ (z – distance from the leading edge, C – chord length).

Experimental apparatus

The experimental set-ups for investigations of the airflow generation by the multi-DBD actuator and for the boundary layer flow separation control experiment are presented in Figs. 4a and 4b, respectively.

The multi-DBD actuators were supplied with sinusoidal high voltage (frequency 1.5 kHz) generated by a high voltage amplifier Trek model 40/15 (U_{pp} – up to 80 kV) or by a function generator Trek PM04015A (U_{pp} – up to 20 kV).

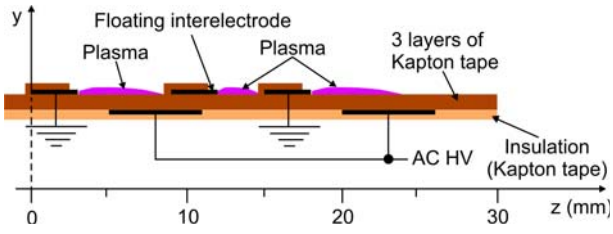

Fig. 3. Schematic side view of the multi-DBD actuator with floating inter-electrode for boundary layer flow separation investigations.

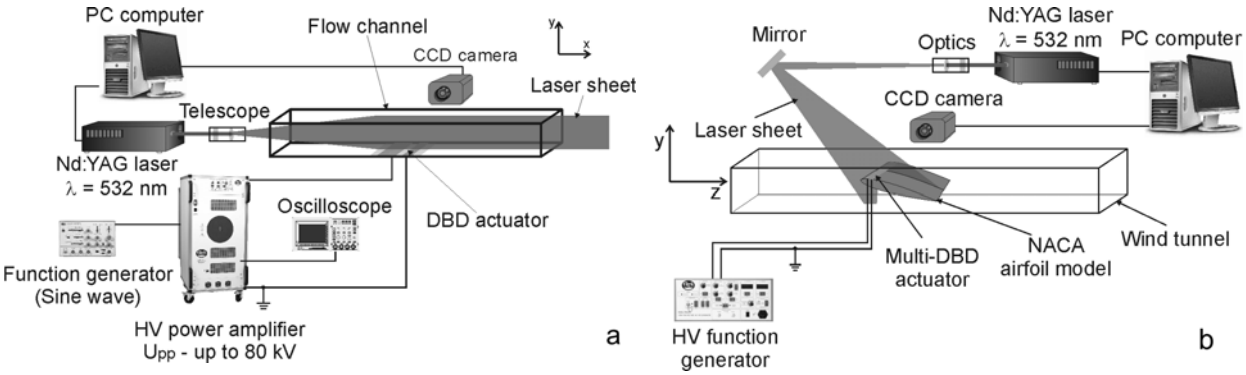

Fig. 4. Experimental set-up for measurements of the airflow generation by the multi-DBD actuator (a) and for the flow separation control experiment (b).

The measurements were carried out in air at atmospheric pressure in an end-opened flow channel (the first stage of the experiment) or in a wind tunnel loop (the second stage of the experiment). The width and height of a test section of the flow channel and the wind tunnel was 200 × 100 mm and 600 × 480 mm, respectively. The 2-D PIV technique was used to take 150 pairs of instantaneous images. Basing on these images, the instantaneous flow velocity fields and the time-averaged flow velocity fields were computed.

Results

The first stage of the experiment

In Fig. 5 the horizontal time-averaged flow velocity profile taken 0.3 mm above the dielectric surface and the time-averaged flow velocity vector field are presented. As it can be seen, the presented multi-DBD actuator with floating inter-electrodes generated airflow up to 8 m/s. The backward flow or vortexes, which could occur in multi-DBD actuators [1, 2], were not observed in this case.

Our goal in the first stage of the experiment was to develop DBD-actuator which will produce higher airflow velocity than a typical DBD actuator (airflow velocity induced by a typical DBD actuator is below 5 m/s). Investigated multi-DBD actuator with floating inter-electrodes was capable to generate significantly higher airflow velocity. Therefore, we expected that it will be attractive for aerodynamic applications, what was examined in the second stage of our experiment.

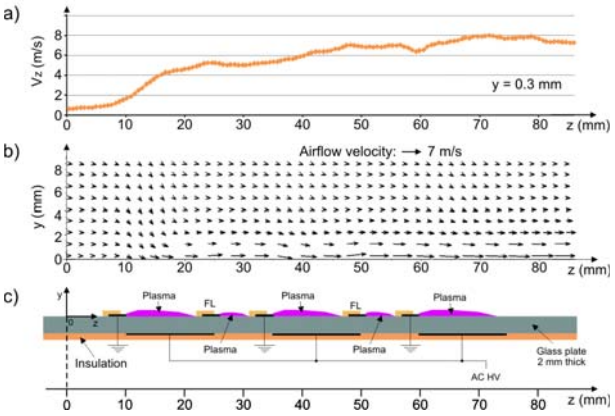

Fig. 5. Time-averaged horizontal flow velocity profile taken 0.3 mm above the dielectric surface (a) and the flow velocity vector field (b) of the airflow generated by the multi-DBD actuator (c). The applied sine-wave voltage was 32 kV_{pp}, the frequency – 1.5 kHz. FL – floating inter-electrode.

The second stage of the experiment

The examples of the time-averaged flow velocity vector fields obtained for the leading edge flow separation control experiment (with the NACA0012 airfoil model) are presented in Fig. 6. In this case the free stream ve-

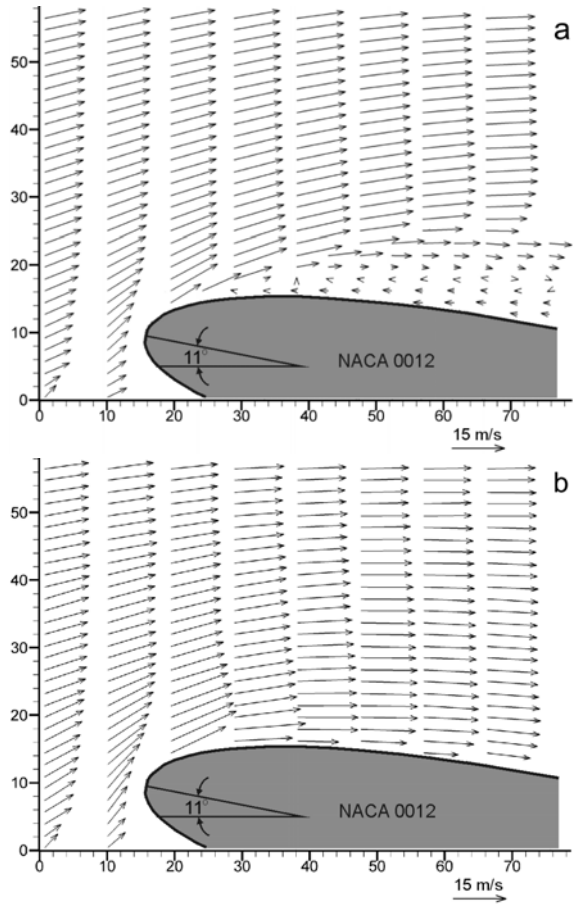

Fig. 6. Time-averaged flow velocity vector field of the airflow around NACA0012 airfoil model for the leading edge flow separation control experiment with the multi-DBD actuator turned off (a) and turned on (b). The main flow velocity was 15 m/s and the angle of attack was 11 degrees. The applied sine-wave voltage was 15 kV_{pp}, and frequency 1.5 kHz.

locity was V_0 = 15 m/s (Re = 2 × 10^5) and an angle of attack was 11°. The observation area was 77 × 57 mm and a spatial resolution of the obtained velocity vector fields was 1.2 × 0.6 mm. As it can be seen, when the multi-DBD actuator was turned off (Fig. 6a) the airflow was separated near the leading edge of the airfoil (stall regime). However, when the high voltage was applied (U_{pp} = 15 kV, frequency 1.5 kHz) to the multi-DBD actuator reattachment of the airflow occurred (Fig. 6b).

Summary

In this paper the innovative multi-DBD actuator with floating inter-electrode was presented and investigated. For the measurements of the airflow produced by the multi-DBD actuator and investigations of the leading edge flow separation control around NACA0012 airfoil model, the 2-D PIV method was used.

The results obtained showed that the airflow generated by the multi-DBD actuator was almost constantly accelerated by consecutive DBD discharges and no backward flow or vortexes were observed. The maximum value of the produced airflow velocity was 8 m/s.

The leading edge flow separation control investigations showed that our multi-DBD actuator is capable of postponing the airfoil stall point. Thus, this actuator can be attractive for aerodynamic applications and should be further developed.

Acknowledgment. The research presented in this paper received funding from the European Community, 7th Framework Programme FP7/2007-2013 under grant agreement no. 234201 (PLASMAERO – Useful PLASMas for AEROdynamic control www.plasmaero.eu) and was supported by the R. Szewalski Institute of Fluid-Flow Machinery, Polish Academy of Sciences, Gdańsk.

References

1. Benard N, Mizuno A, Moreau E (2009) A large-scale multiple dielectric barrier discharge actuator based on an innovative three-electrode design. J Phys D: Appl Phys 42:235204
2. Forte M, Jolibois J, Pons J, Moreau E (2007) Optimization of a dielectric barrier discharge actuator by stationary and non-stationary measurements of the induced flow velocity: application to airflow control. Exp Fluids 43:917–928
3. Jolibois J, Forte M, Moreau E (2008) Application of an AC barrier discharge actuator to control airflow separation above a NACA0015 airfoil: optimization of the actuation location along the chord. J Electrostat 66:496–503
4. Moreau E (2007) Airflow control by non-thermal plasma actuators. J Phys D: Appl Phys 40:605–636
5. Sosa R, Artana G, Moreau E, Touchard G (2006) Flow control with EHD actuators in middle post stall regime. J Braz Mech Sci Eng Soc 28:200–207